GEODYNAMICS & TECTONOPHYSICS
Published by the Institute of the Earth's Crust, Siberian Branch, Russian Academy of Sciences

TECTONOPHYSICS

2023 VOLUME 14 ISSUE 5 ARTICLE 0720

ISSN 2078-502X

DOI: 10.5800/GT-2023-14-5-0720

MODELING OF THE LITHOSPHERE IN THE WHITE SEA REGION USING DECOMPOSITION OF ANOMALOUS GRAVITATIONAL AND MAGNETIC FIELDS

B.Z. Belashev, L.I. Bakunovich ✉, N.V. Sharov

Institute of Geology, Karelian Research Centre of the Russian Academy of Sciences, 11 Pushkinskaya St, Petrozavodsk 185910, Russia

ABSTRACT. The research area includes the White Sea and adjacent land located in the junction zone of the eastern part of the Fennoscandian Shield and the Russian Plate. The purpose of the study is to construct a model of the lithospheric structure of the region using decomposition of anomalous gravitational and magnetic fields and inverse problem solving for components of gravity and magnetic fields, respectively. The decompositions of the fields were provided by the singular spectral method in the software package "R 4.3.1". The inverse problems were solved using the programs of the "Integro" complex. The components of the fields help to identify and analyze buried geological structures. The rift system of the White Sea is most clearly represented by the fourth component of the gravitational and magnetic fields. The positions of density and magnetic inhomogeneities of the Earth's crust corresponding the components of the fields have been determined. The component model is compared with the seismic density and magnetic models of the lithosphere along the 3-AP geotraverse (Kem – White Sea Throat).

KEYWORDS: White Sea; lithosphere; rift system; gravitational and magnetic fields; density; magnetic susceptibility; seismic density and magnetic models; singular value decomposition; "R4.3.1" and "Integro" software products

FUNDING: The study was funded from the budget of KarRC RAS (Institute of Geology).

RESEARCH ARTICLE

Correspondence: Lyubov I. Bakunovich, luba5_89@mail.ru

Received: February 17, 2023
Revised: May 10, 2023
Accepted: May 12, 2023

FOR CITATION: Belashev B.Z., Bakunovich L.I., Sharov N.V., 2023. Modeling of the Lithosphere in the White Sea Region Using Decomposition of Anomalous Gravitational and Magnetic Fields. Geodynamics & Tectonophysics 14 (5), 0720. doi:10.5800/GT-2023-14-5-0720

1. INTRODUCTION

The paper presents the modeling results for the White Sea area and adjacent land located in the junction zone of the eastern Fennoscandian Shield and the sediment-covered Russian Plate. Geodynamics of the region is determined by continuous postglacial shield uplift, flow of the upper mantle from the Barents Sea basin underneath the continental crust, influence of spreading pressure for the Arctic and Atlantic Mid-Ocean ridges, and change in the Earth's rotation regime [Kutinov, 2021]. The features of the lithospheric structure and dynamics contribute to the study of the relationships between continental rifting, intraplate and kimberlite magmatism, and oil and gas content [Kearey et al., 2009]. The regional geological studies are aimed at searching for hydrocarbons, kimberlite pipes, and other useful minerals [Kazanin et al., 2006; Aplonov, Fedorov, 2006].

The fundamental and search problem solving is assisted by the lithospheric structure models based on the results of seismic, gravimetric and magnetometric surveys [Kheraskova et al., 2006; Zhuravlev, 2007; Lisitsyn et al., 2017]. A priory information of the models is mainly assigned by the seismic profiling data. The comparison between the costs of using methods in large areas shows that aeromagnetic and gravimetric surveys are most effective.

The paper continues a series of works on deep-structure modeling of the White Sea area [Sharov et al., 2020a, 2020b; Nilov et al., 2021]. The lithospheric models based on airborne gravity and magnetic survey data with using components of anomalous gravitational and magnetic fields are consideration. Decomposition of fields and inverse problem solving for their components make it possible to perform a more detailed and deeper analysis of the field structures, to determine spatial location of corresponding sources, and to assess density and magnetic susceptibility of their constituting rocks.

Stages of the modeling process include decomposition of anomalous gravity field in Bouguer reduction and anomalous magnetic field reduced to the pole, location and visualization of the component-corresponding rock distributions, and comparison between the results obtained and those already available. Modeling was performed using computer algorithms and technologies. Potential fields were decomposed with singular value decomposition [Gantmakher, 2010], minimally involving the prior information and providing a high-quality reconstruction of the simulated signals and images.

2. MATERIALS AND METHODS

2.1. Initial data

The initial gravimetric data are represented by a fragment digital map of the gravitational field scale 1:1000000 in Bouguer reduction, built on the basis of gravity survey data [State Geological Map..., 2009a, 2009b]. Analyzed map fragment on a scale of 1:250000 with dimensions of 427×497×3 pixels is shown in Fig. 1, a. Geotraverses 4B (Kostomuksha – Kem) and 3-AP (Kem – Gorlo of the White Sea) [Sharov et al., 2010] are shown by black lines.

A similar fragment is highlighted in the digital matrix of the general magnetic intensity (cell 500×500 m), constructed from the data basic aeromagnetic surveys [State Geological Map..., 2009a, 2009b, 2009c], reduced to the pole [Nilov et al., 2021] (Fig. 2, a).

The fragment contains Onega-Kandalaksha, Keretsko-Pinezhsky, Chapomsko-Leshukonsky, Mezensky paleorifts of northwestern prostrations. Rifts are separated by intertrough bridges and ledges crystalline basement, covered by the waters of the White Sea and platform sedimentary formations [Baluev et al., 2009].

Geotraverse 3-AP crosses rifts, gravity and magnetic anomalies. Data processing of it's RWM-CDP, CDPM, DSS profiles and other results of seismoacoustic profiling were used in construction of seismic density and magnetic models of earth's crust of the region [Sharov et al., 2020a; Belashev et al., 2020].

2.2. Data processing methods

The gravitational and magnetic fields of the fragment were decomposed with algorithm of 2D singular spectrum analysis (2D-SSA). Based on the initial 2D field distribution and two-dimensional scanning window of size L, the algorithm forms a trajectory rectangular Hankel matrix H and finds the eigenvalues $\lambda_1 \geq ... \geq \lambda_d \geq 0$ of a square matrix D=H·H' and their corresponding eigenvectors U_1, ..., U_d, where d=max{j:λ_j>0}, and vectors $V_j = H'U_j \Big/ \sqrt{\lambda_j}$, which are used for calculation of the components of singular value decomposition of field $X_j = \sqrt{\lambda_j} U_j V_j'$.

The basis of decomposition is determined automatically. A small number of positive eigenvalues due to a low-rank matrix D provides effective methods for data compression and selection signal and noise components of the field.

A 2D-SSA module is a part of RSSA package in the freely distributed R 4.3.1 software product [Golyandina et al., 2015]. The size of scanning window L was 75×75 pixels.

Solving inverse problems involves software complex "INTEGRO" [Cheremisina et al., 2018] using the regularization, interpolation and extrapolation methods. The calculations were made over two- and three-dimensional grids using improved spectral algorithms of fast Fourier transform [Priezzhev, 2005], which do not produce artifacts caused by lateral limitation and non-periodicity of the data [Mitsyn, Ososkov, 2016].

Correlation coefficients for the fields and their components were calculated using corr2 function in MATLAB system [Statistics Toolbox..., 2005]. For the images with the distribution of data differing in χ^2 criterion from normal distribution, the significance of the matrix correlation coefficients was assessed using the Kolmogorov-Smirnov test (KS test) [Gavrilov, 2013].

3. RESULTS

Fig. 1 and Fig. 2, drawn for anomalous gravitational and magnetic fields, show the maps of the fragment (a) and their singular value decomposition components for eigenvalues (b–f).

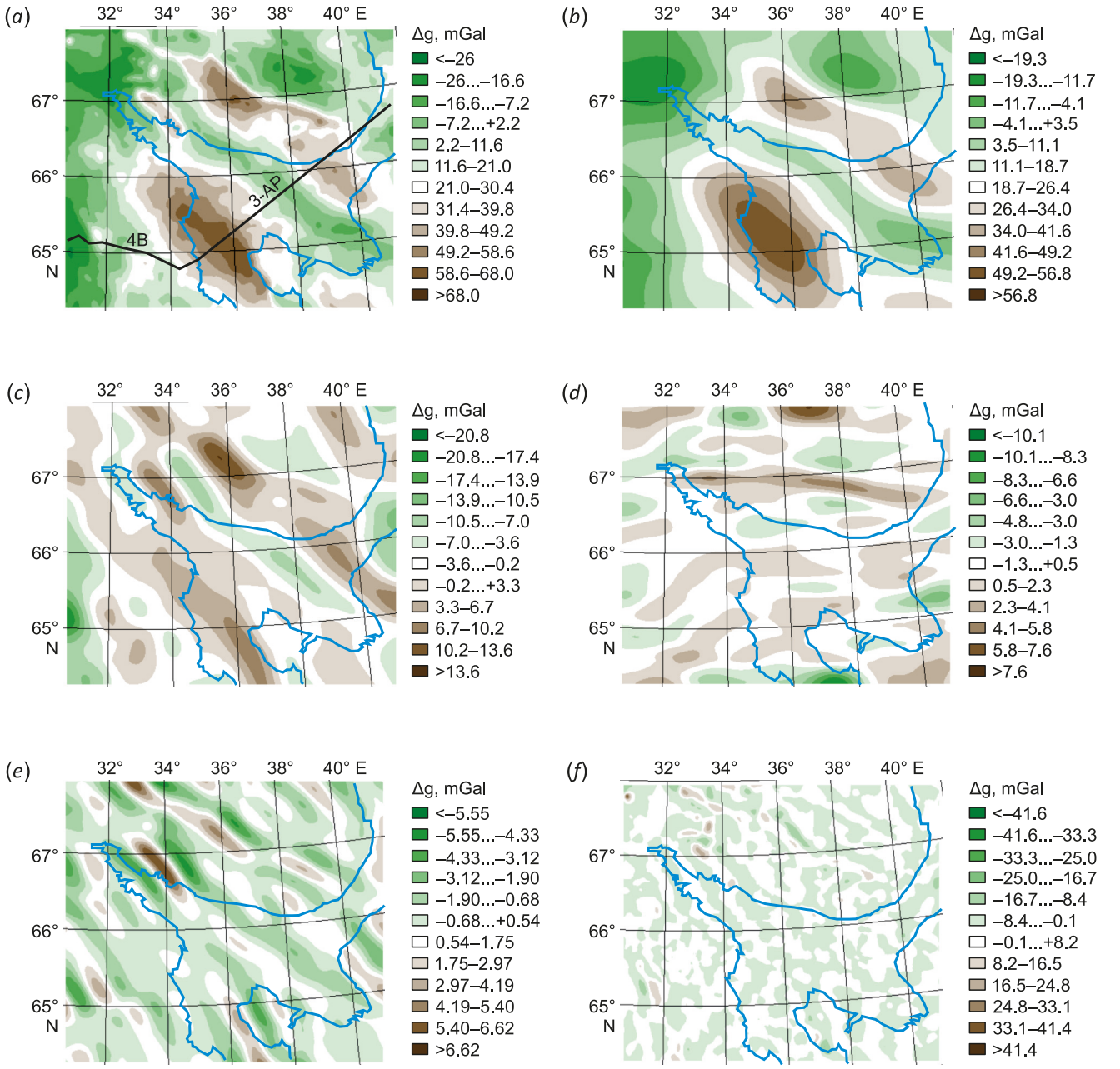

Fig. 1. A fragment of the digital map of an anomalous gravity field (*a*) and the first five components of its singular value decomposition (*b–f*).

Fig. 3 shows a tectonic scheme of the White Sea paleorift system.

Fig. 4 represents eigenvalues of singular decomposition for the processed gravitational- and magnetic-field fragments characterizing energies of components. The first five components of decomposition of the gravity field account for about 70 % of the field energy.

Table 1 presents correlation coefficient *r* for the gravity field of the fragment and for its successively summed first five components.

The components of an anomalous gravity field of different eigenvalues in Fig. 1, b–f are characterized by energy and spatial frequencies. The first, highest-energy component (b) has two large positive anomalies and their separating negative gravity anomaly which falls within a wide zone near the Keretsk-Pinega rift. Field components (c–e) of the eigenvalues numbered 2–4 have similar energies. Components (c, d) are dominated by positive gravity anomalies and components (e, f) – by negative gravity anomalies. The anomalies of components (c, e) are oriented northwestwards and those of component (d) are oriented in the eastern and northeastern directions. These directions correspond to the strike of the Kandalaksha-Onega and Zimnegorsk faults. Most of the smaller negative gravity anomalies of component (f) are oriented in the same directions.

In the first component of the magnetic field of the fragment (see Fig. 2, b), large positive and negative anomalies

are elongated to northwest and west. The second component of the magnetic field of the fragment represents the merged positive anomalies of the northwestern orientation (c). In the third component, the magnetic anomalies are surrounded by northwest-oriented oval structures, located regularly in the northeastern direction too (d). This and the next components are dominated by negative magnetic anomalies. Small magnetic anomalies of the fourth component, as for as gravity anomalies, trace the White Sea rift system elements and are located regularly in the northern direction (e). Rare positive anomalies in the decomposition residue are pointwise (f).

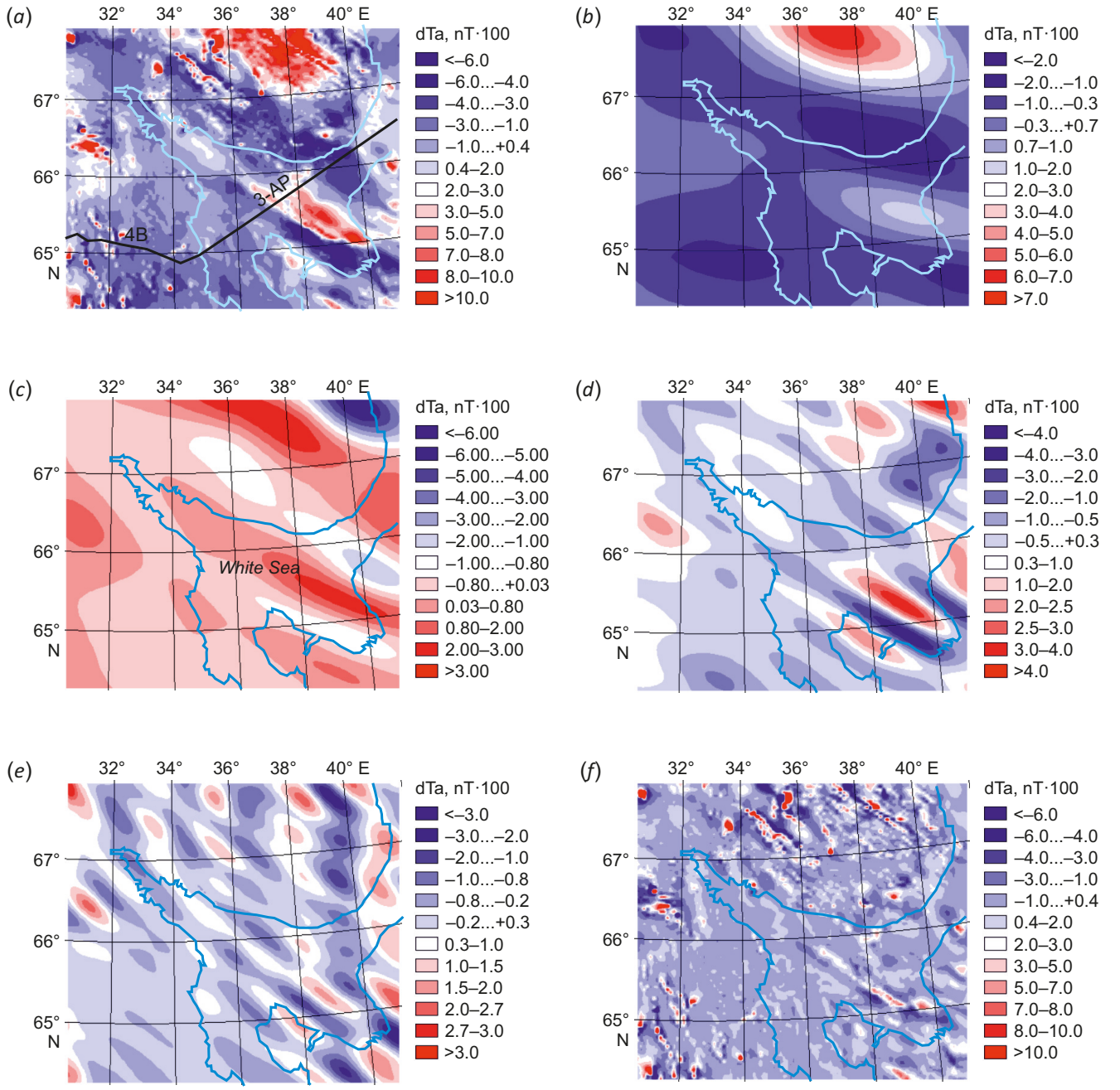

Fig. 2. A fragment of the digital map of an anomalous magnetic field (*a*), the first four components (*b*–*e*) and the residue (*f*) of its singular value decomposition.

Table 1. Correlation coefficients for the gravity field of the fragment and its components

Components	1	1+2	1+2+3	1+2+3+4	1+2+3+4+5	Residue
r	0.82	0.91	0.94	0.95	0.96	0.32

Note. Last column contains correlation coefficient for the initial field and decomposition residue.

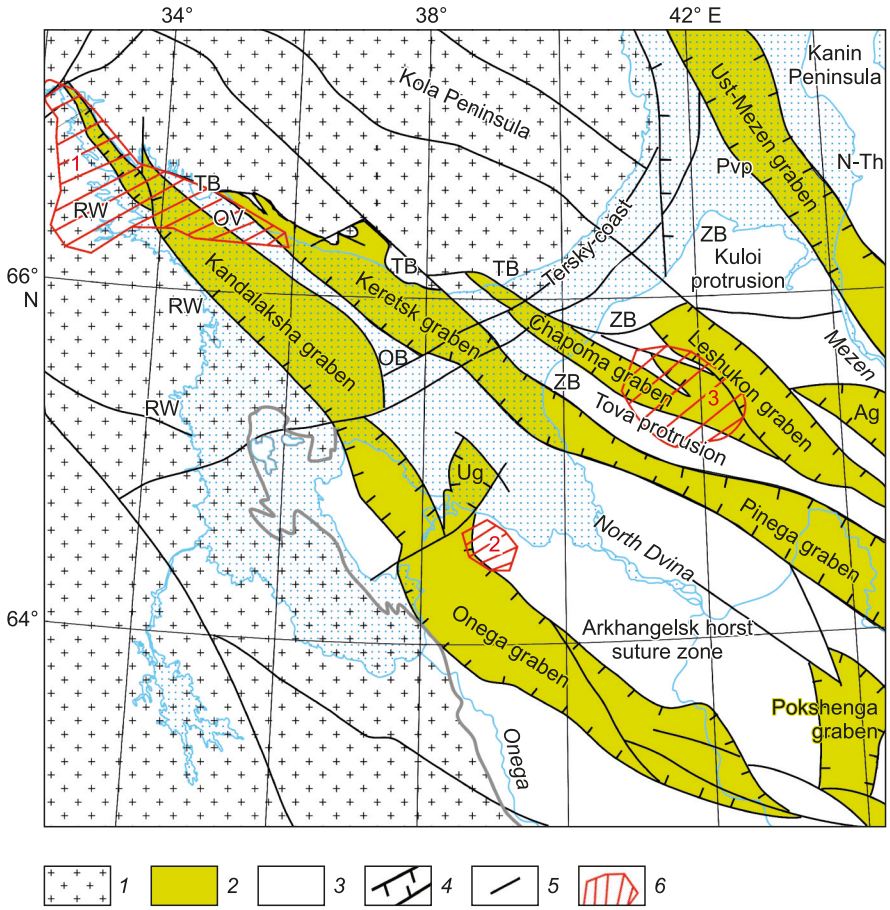

Fig. 3. A tectonic scheme of the White Sea paleorift system [Sharov, 2022, p. 50, 68].
Pvp – Ponoy basin, N-Th – Nessko-Tylugsky horst, Ag – Azopol graben, Ug – Unsky graben, TB – Tersky Coast, ZB – Winter Coast (Zimniy Bereg), OV – Olenitsky bar. *1* – Early Precambrian complexes of the Fennoscandian Shield; *2* – terrigenous complex of the Riphean rocks which act to fill the rift depressions; *3* – Vendian-Paleozoic platform cover, overlapping the rift depressions; *4* – fault limitations of rift grabens; *5* – other faults; *6* (RW) – areas of manifestations of the Middle Paleozoic alkaline magmatism of the tube-dike type: 1 – Kandalaksha, 2 – Nenoksky, 3 – Zimneberezhny.

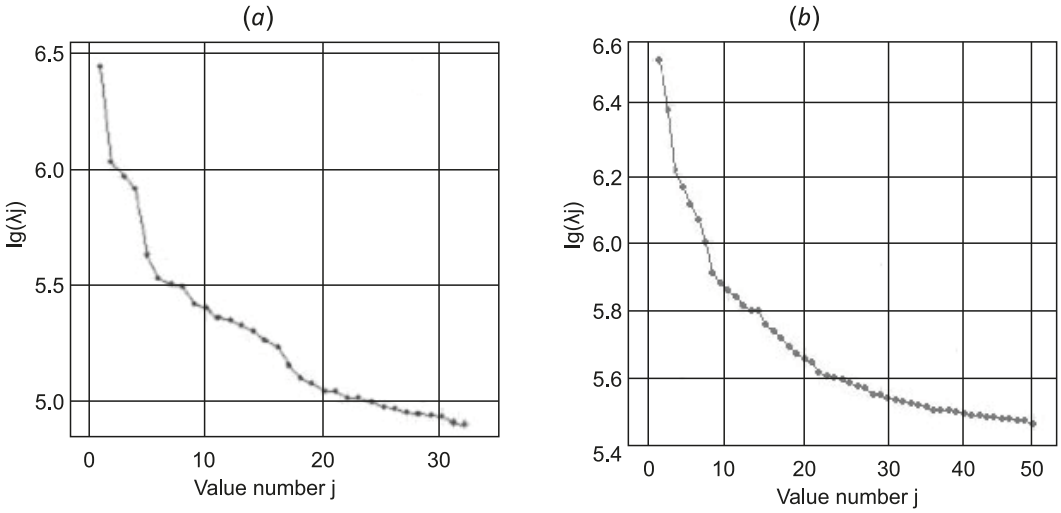

Fig. 4. Eigenvalues of the singular value decomposition of anomalous gravity (*a*) (see Fig. 1, a) and magnetic (*b*) (see Fig. 2, a) field fragments.

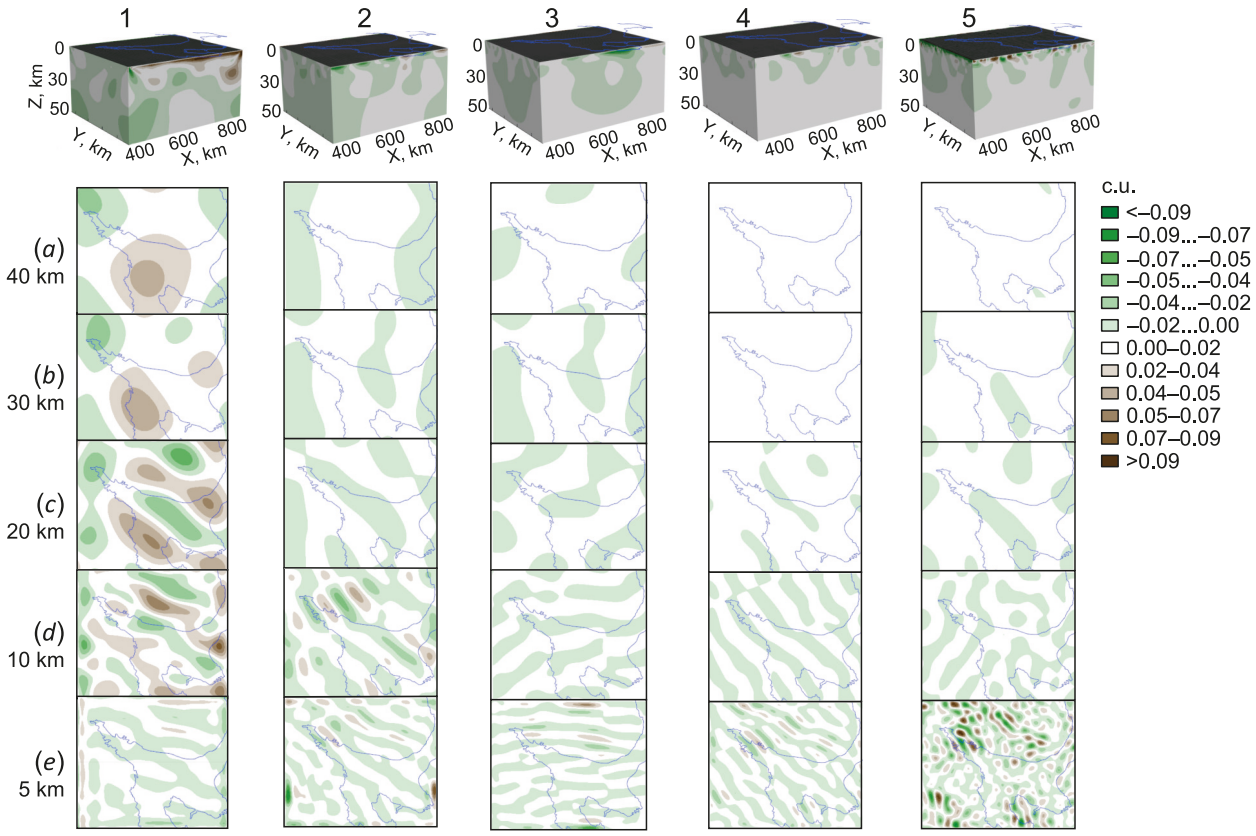

Fig. 5. 3D conditional density distributions for the first five components (1–5) of the singular value decomposition of the anomalous gravitational field and its horizontal sections for depths of 40 (*a*), 30 (*b*), 20 (*c*), 10 (*d*) and 5 km (*e*).

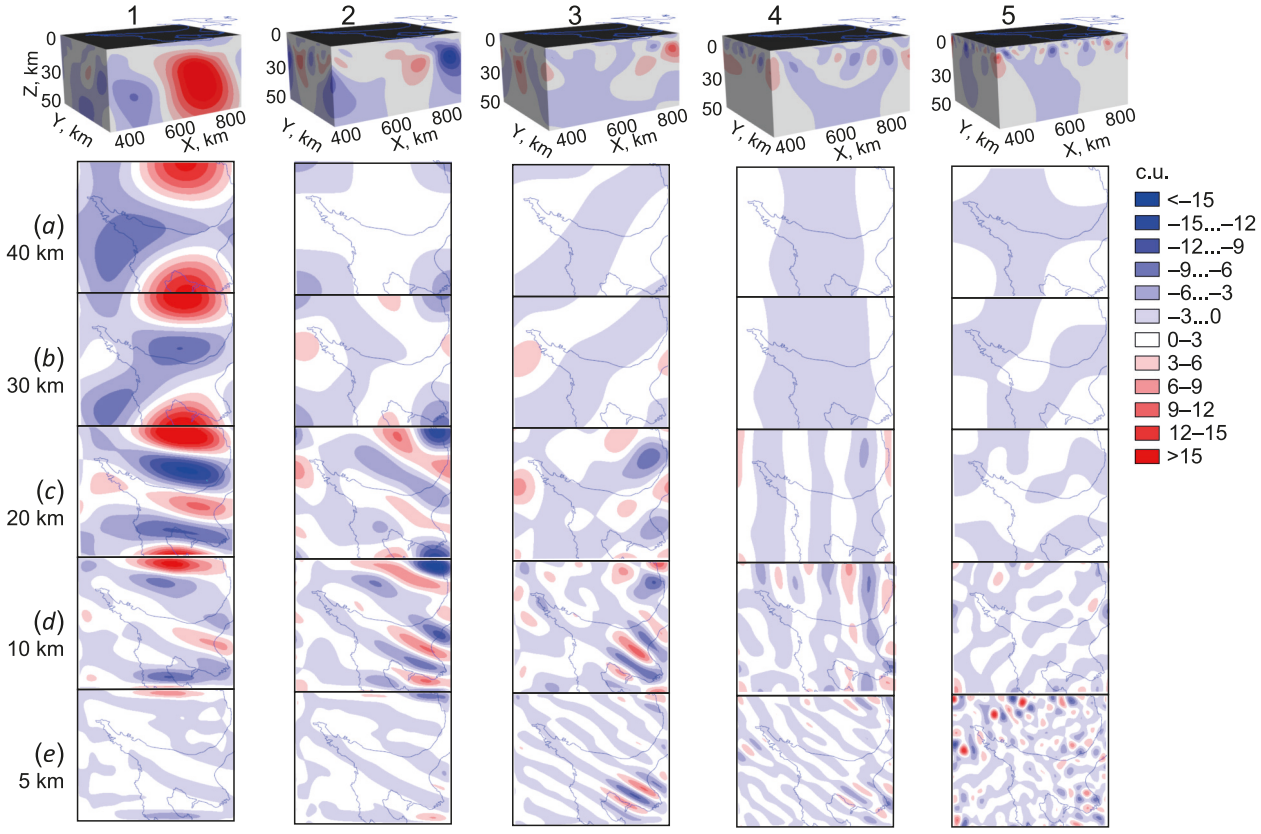

Fig. 6. 3D distributions of conventional magnetic susceptibility of the first four components (1–4) and residual singular value decomposition of the anomalous magnetic field (5) and its horizontal sections for depths of 40 (*a*), 30 (*b*), 20 (*c*), 10 (*d*) and 5 km (*e*).

Fig. 5 and Fig. 6 show respective 3D distributions of conventional density of the first five anomalous gravity field decomposition components and conventional magnetic susceptibility of four components, and residual decomposition of an anomalous magnetic field.

The locations of field component anomaly sources in the lithosphere are visualized in cross-sections at depth of 40 (a), 30 (b), 20 (c), 10 (d) and 5 (e) km.

The density distribution in the first anomalous gravity field decomposition component, almost centrosymmetrical at a depth of 40 km (1a), is added up by a new cluster at a depth of 30 km (1b), thus becoming asymmetric and slightly elongated to the northwest. The northwest extension intensifies at a depth of 20 km (1c), with the clusters multiplied and separated from each other and the crustal extension zone initiated near the Keretsk-Pinega graben. The density distribution becomes even more detailed at a depth of 10 km (1d). A further northwestward extension complements the shear along the axial line of the White Sea Throat: the areas of compression and extension

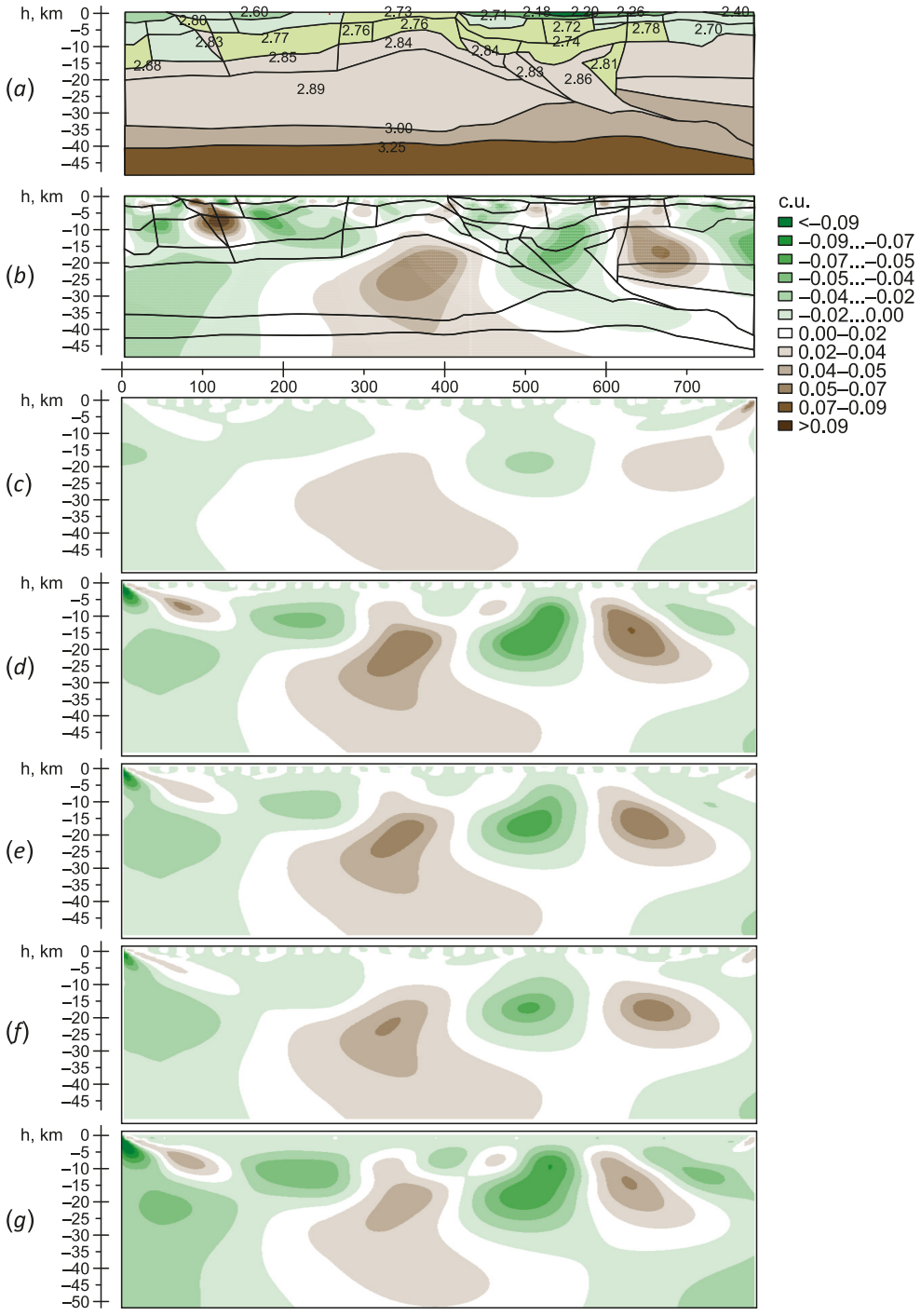

Fig. 7. Lithospheric models compiled along the 3-AP geotraverse: (*a*) – seismic density model; (*b*) – gravity model; (*c–g*) – gravity models for successive summation of the first five gravity field components.

occurring therein correspond to horsts and grabens of the White Sea rifts. At a depth of 5 km (1e) there are only the extension zones.

For components 2–5 the extension areas are dominated in all sections. For components 2 and 3 density distributions symmetric to the axis the south-to-north at depths of 30–40 km, turn respectively to the northwest and northeast at a depth of 20 km.

In a 10 km deep cross-section, the decompaction zones divide and and multiply, elongating in the above-mentioned directions and decreasing in size perpendicularly thereto.

For component 3 is dominated by the northeast- and east-oriented extension zones. This trend can still be observed in a 5 km deep section, with the extension zones more and more oriented towards the west and east, respectively.

For components 4 and 5 of gravity field the sources of density anomalies have almost no in the lower crustal horizons. They manifest themselves ubiquitously at depths

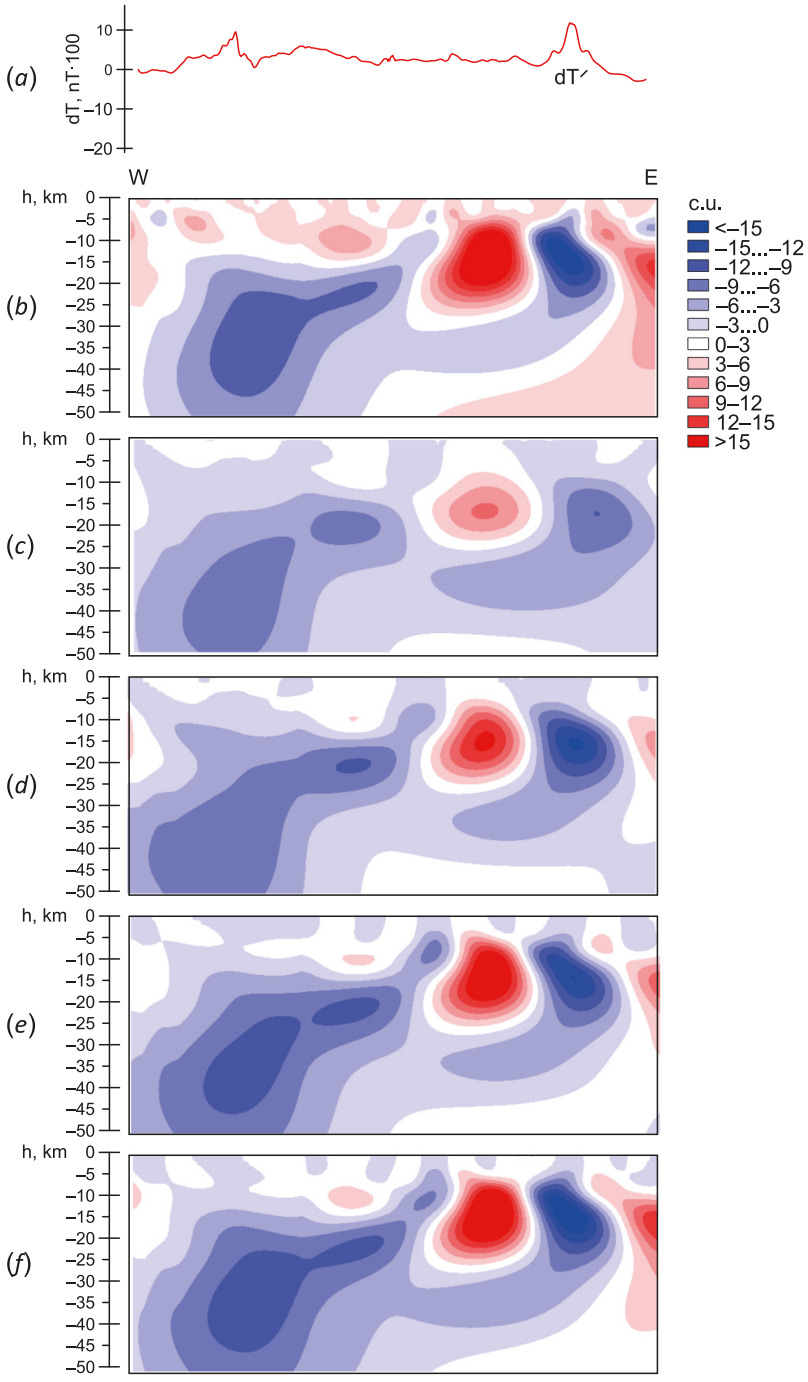

Fig. 8. Overlapping initial and model distributions of the anomalous magnetic field along the 3-AP geotraverse (*a*), 2D distribution of conventional magnetic susceptibility in the magnetic model (*b*) and similar 2D distributions for successively summed 1–4 anomalous magnetic field decomposition components, (*c*–*f*).

of no less than 20 km. The density distribution in component 5 at a depth of 10 km is dominated by the northeast-oriented extension zones. The density distribution acquires a mosaic pattern at a depth of 5 km. The alternating positive and negative density deviations are clustered in the areas of Kostomuksha, Onega Peninsular, upper Kandalaksha graben, and along the Kolmozero-Voronya suture zone.

The distribution of conventional magnetic susceptibility for the first anomalous magnetic field component shows vertical southeastern and northeastern magnetization structures at depths of 20–40 and 5–40 km, respectively, and magnetic anomaly beneath the Keretsk graben at depths of 5–20 km (Fig. 6, 1a–e). Such distributions for the second and third components show that lower-intensity and smaller in the sizes magnetic field sources are located at depths of 10–30 km and oriented primarily to the northwest (Fig. 6, 2, 3 b–d). Small magnetic sources in the distribution for the fourth-component are located at depths of 5–10 km and oriented northwards (Fig. 6, 4d). For decomposition residue the distribution shows point magnetic field sources in a 5 km deep cross-section, concentrated primarily in the northwest and southeast (Fig. 6, 5e).

Fig. 7, a, b, represents seismic-density and gravity models of the lithosphere built along the 3-AP geotraverse with regard to the block structure (a) and with no regard to it (b) [Sharov et al., 2020a].

Fig. 7, c–g, shows the distributions of conventional density in successive summation of the first to five gravity field components.

Fig. 8 shows anomalous magnetic field distribution along the 3-AP geotraverse (a), 2D distributions of conventional magnetic susceptibility (b) of the magnetic model [Nilov et al., 2021], and their distributions for 1–4 singular value decomposition components of magnetic field, similar to those in Fig. 7, c–f.

4. DISCUSSION

Singular value decomposition produces the distributions of empirical modes. Its principal advantage lies in the search of the basis of decomposition directly from the processed data. Such basis is formed automatically with regard to specific features and inner structure of the data and is characterized as completeness, orthogonality, locality, and adaptability. The obtained modes describe changeability of a signal and allow to determine their relative contribution to a signal. The modes selected based on eigenvalues (spatial frequencies, energies) and eigenvalue groups make it possible to distinguish trends, noises, and other distribution features. Due to these, decomposition can reduce the dimensionality of a dataset and simplify its interpretation. Empirical mode decomposition is used in the analysis of multidimensional data arrays in meteorology, oceanology, and atmospheric physics [Elsner, Tsonis, 1996; Navara, Simoncini, 2010]. However there is a need for more practically oriented studies in the field of geophysics, geomorphology, and geoinformatics [Korotchenko, 2013].

Empirical mode decomposition is also performed using the Hilbert-Huang transform [Huang, Samuel, 2005; Dolgal, Khristenko, 2017; Kalinin et al., 2019; Diuk et al., 2018]. Boundary errors arising during the signal reconstruction due to the use of spline interpolation [Dolgal, Khristenko, 2017] and the lack of proven algorithms for 2D distribution processing make the choice of singular value decomposition to decompose the anomalous gravitational and magnetic fields more preferred.

Fig. 1 and Fig. 2, b–f, show that eigenvalue-ranked decomposition components differ in spatial frequency and describe the size, direction, sign and association of anomalies in different ways. Positive gravity anomalies for decomposition components are assigned to consolidated segments of the lithosphere, negative anomalies – to the extension, shear and rock deconsolidation zones. Positive magnetic anomalies reflect the presence of ferromagnetic minerals, such as magnetite, in the rock composition. The magnetic susceptibility decreases with depths as the Earth's interior temperature rises. For the studied low heat flow area, the Curie isotherm of magnetite 584 °C is considered to be in the mantle, and the magnetoactive layer is considered to be within the Earth's crust [Wasilewski, Mayhew, 1992].

Low-frequency components of potential fields are traditionally related to the deep-seated crystalline basement structures, high-frequency components – to the upper crustal sources.

The most obvious relationship between the gravity anomalies and the White Sea rift system is represented by the fourth field component (see Fig. 1, e). Its positive anomalies trace the Kandalaksha, Onega, Keretsk, Pinega, Unsky, Leshukon, Chapoma and Maloushika grabens and the Ponoy basin, with the positive anomalies related to intrabasinal highs and crystalline basement protrusions. A similar function is performed by negative anomalies of the fourth magnetic field decomposition component (see Fig. 2, e).

The structure of the White Sea rift system reveals the common features of continental rifting: the presence of a permanent source of the mantle substance, extensive rift forming troughs, accommodational highs which separate rift grabens and half-grabens, rift displacement relative to protruding mantle, and a thinned continental crust beneath the rifts. A special feature of the paleorift system of the White Sea is its long development during 1.3 Ga, related to the marginal-continental position of the system and its sensitivity to geodynamic transformations, in accordance with the plate tectonic models [Baluev et al., 2000].

In formation of the White Sea rift system there are distinguished the Paleoproterozoic (1.3–1.2 Ga) formation of the Baltic continental margin, the Late Riphean extension of the Timan margin of the Baltic after the super-continent Rodinia disintegration and the paleo ocean Japetus opening, the Devonian activation of the system caused by the Japetus closure, initiation of the East Barents rifting trough, and the Late Cenozoic formation of the present-day, Riphean rift-related White Sea tectonic basins assigned to

the formation time of the North Atlantic and Arctic oceans. The presence of the source of mantle substance and the channel through which it intrudes into to the Earth's crust is evidenced by the central consolidated area on the analyzed models in Fig. 5 (1a) and Fig. 7. The channels which relate it to the apophyses are not visible at large and moderate depths. They are indicated by converging disintegration zones in Fig. 7. The channels are visualized in the near-surface areas with high spatial resolution.

The distributions of conventional magnetic susceptibility in Fig. 6 are in partial agreement with the model results for the three-layer magnetoactive layer of the Onega – Kandalaksha paleorift and the White Sea Throat [Baluev et al., 2018]. Magnetic sources at depths of 10–30 km can be assigned to the lower level related to the Middle and Upper Riphean rifting of the White Sea mobile belt, associated with the main Riphean-Vendian volcanic occurrences. The sources in the depth range from 1 to 10 km can be considered as a result of the Middle Paleozoic (Late Devonian) reactivation of the White Sea rift system with alkaline-ultrabasic magmatism occurrences. In the upper crust such sources are often represented by alkaline dike swarms and diatremes. No comparison was made between the upper level of the 0.2–1.0 km deep magnetoactive layer and the modeling data because of the depth discretization with a 1 km depth interval in the component model.

Figs 5, 6, 7, 8 show the incompatibility between the ranges of maximum conventional density and magnetic susceptibility values of the rocks. Most of the magnetic sources are confined to the moderate- and low-density areas.

The lower part of the central, consolidated area (see Fig. 7, d, e, g) is oriented to the northwest, the middle part – to the northeast, and its small upper part – to the northwest; the intermediate parts have sublatitudinal strike. If all these parts reflect the stages in the formation of the White Sea rift system, they could be used to estimate the substance volumes entering the Earth's crust at each stage.

Consolidation in some parts of the lithosphere is associated with extensional, ductile, bending and brittle deformations in the other, adjacent parts (see Fig. 7, a). The supply of portions of the mantle substance and the formation of consolidated parts in the crust surface layers cause the occurrence of new and deepening of the pre-existing deconsolidation zones, their merging, and rift formation. The rifting mechanisms are considered in [Tevelev, Fedorovsky, 2016; Kazmin, Byakov, 1997; Baluev et al., 2021].

Fig. 7 and Fig. 8 illustrate an agreement between the results of seismic density, magnetic and component modeling along the 3-AP geotraverse and the relationship between deep-seated and near-surface lithospheric structures in the region. Fig. 7 shows the features of continental rifting: crustal bending above the central, consolidated area, compensated Moho uplift in the area of the Keretsk-Pinega rift, and thinned continental crust therein. The surface deconsolidation zones are related to similar large underlying zones. The similarity can be due to deep degasation through these structures.

In Fig. 8, a, b, it can be seen that clearly defined positive magnetic anomalies are caused by near-surface magnetic sources. Deeper sources contribute to the regional component of the magnetic field. A decay of the magnetic induction field with distance from the source, sharper than that of the gravitational field, complicates their localization in the lithosphere. This is especially true for the locations of the lower edges of magnetic sources. The magnetic and component models, which involve solving the inverse problem, cope with this task. Approximate locations of large magnetic sources in the lithosphere can be reliably determined already from the first mode decomposition. The process of successively summing up the components does not fundamentally change the pattern of magnetic sources but adds some details thereto.

When Fig. 7 is compared to Fig. 8, it is apparent that an extended magnetic source falls within the deconsolidation zone at depths from 30 to 5 km. The zone-infill low-density and high magnetic-susceptibility material may include serpentinites which occur as a result of the effect of water on ultrabasic rocks – dunites [Komarov, 1965]. Magnetite produced by olivines from dunites gives serpentinites magnetic susceptibility of 0.15 at their average density of about 2600 kg/m^3. Serpentinization produces hydrogen that reduces metal oxides and forms degasation and heat flows. Serpentine instability at temperatures higher than 400 °C determines the upper depth limit for its occurrence in the crust. Based on heat flow estimates of 10–50 mW/m^2 for the studied region and 3D geothermal modeling results [Tsibulua, Levashkevich, 1992; Khutorskoy et al., 2013], isotherm 400 °C corresponds to depths of 20–30 km. The evidence for serpentinization is a rock massif in the southern White Sea. Ultrabasites of the Razostrov Island are represented by serpentized dunites and harzburgites [Stepanov, Stepanova, 2007].

Another aspect of serpentinization is related to the effect of carbonic-acid water on mantle peridotites, pushed down into the Earth's crust along the faults. Methane and hydrocarbon compounds formed in the course of the reaction accumulate in the serpentinization zones and migrate through the degasation channels [Raznitsin et al., 2020]. The supply of the zones with new portions of mantle substance makes such hydrocarbon source renewable. As seen from Fig. 7 and Fig. 8, such zones can be easily searched through comparison between 3D and 2D gravitational and magnetic models, and quantitative assessments of location and content of the sources can be obtained using the singular value decomposition components of geophysical fields.

5. CONCLUSION

3D component lithospheric model of the White Sea region used the aerial survey and performs decompositions of anomalous gravitational and magnetic fields by the algorithm of singular spectral analysis and solves inverse gravimetric and magnetic problems for the field components, thus obtaining corresponding distributions of conventional density and magnetic susceptibility in the crustal volume.

The advantage of this approach is the studied-field compatible, automatically formed basis of decomposition with properties of completeness and orthogonality.

The singular value decomposition components adequately reflect the structure of anomalous gravity and magnetic fields and identify regional and local anomalies differing in location, sign, shape, size, and orientation. Large anomalies correspond to the first, eigenvalue-ranked field components. The White Sea rift system can be fully described by the fourth components of the gravitational and magnetic fields with anomalies tracing grabens, half-grabens, and intrabasinal highs. The field components with large eigenvalue numbers characterize small anomalies in the upper crustal layers, measurement errors, and field reductions.

The distributions of conventional rock density and magnetic susceptibility, corresponding to the anomalous field components, localize the inhomogeneities in the crustal volume and allow estimating their dimensions, shape, orientation and composition, as well as the relationship between the geological structures. The distributions of conventional density in the component model demonstrate structure of the crust in the region, the presence of the mantle-related magma-supply channel beneath the Keretsk and Kandalaksha grabens, orientations of magma intrusions into the Earth's crust and the relationships between them, and the properties inherited by the surface areas from their underlying structures.

Component distributions of conventional magnetic susceptibility of the rocks confirm the stratified structure of the magnetoactive layer of the Earth's crust in the region. The distributions related to the first three decomposition components yield vertical northeast and southeast magnetization directions and a magnetic anomaly beneath the Keretsk rift at depths of 5–30 km. The distributions corresponding to the fourth decomposition component of the anomalous magnetic field describe magnetic sources in a 5–10 km layer, and the decomposition residue distributions – the sources at depths of five kilometers or less. The confinedness of magnetic sources to deconsolidation of the volumes of the crustal material in the region implies the relationship between rifting, intraplate magnetism and serpentinization processes. The 3D component model provides detailed information about the structures of anomalous geophysical fields and their sources. A combined analysis of the density and magnetic modeling results makes it easier to search for promising geological structures, for example, serpentinization zones – potentially renewable deep-seated sources of oil and gas formation in the Earth's crust.

6. ACKNOWLEDGEMENTS

The authors thank the reviewers and the editorial board of the journal for editing and improving the article.

7. CONTRIBUTION OF THE AUTHORS

All authors made an equivalent contribution to this article, read and approved the final manuscript.

8. DISCLOSURE

The authors declare that they have no conflicts of interest relevant to this manuscript.

9. REFERENCES

Aplonov S.V., Fedorov D.L. (Eds), 2006. Geodynamics and Possible Oil and Gas Potential of the Mezensk Sedimentary Basin. Nauka, Saint Petersburg, 319 p. (in Russian) [Геодинамика и возможная нефтегазоносность Мезенского осадочного бассейна / Ред. С.В. Аплонов, Д.Л. Федоров. СПб.: Наука, 2006. 319 с.].

Baluev A.S., Brusilovsky Yu.V., Ivanenko A.N., 2018. The Crustal Structure of Onega-Kandalaksha Paleorift Identified by Complex Analysis of the Anomalous Magnetic Field of the White Sea. Geodynamics & Tectonophysics 9 (4), 1293–1312 (in Russian) [Балуев А.С., Брусиловский Ю.В., Иваненко А.Н. Структура земной коры Онежско-Кандалакшского палеорифта по данным комплексного анализа аномального магнитного поля акватории Белого моря // Геодинамика и тектонофизика. 2018. Т. 9. № 4. С. 1293–1312]. https://doi.org/10.5800/GT-2018-9-4-0396.

Baluev A.S., Kolodyazhny S.Yu., Terekhov E.N., 2021. Comparative Tectonics of the White Sea Paleorift System and Other Continental Rifting Systems. Lithosphere 21 (4), 469–490 (in Russian) [Балуев А.С., Колодяжный С.Ю., Терехов Е.Н. Сравнительная тектоника палеорифтовой системы Белого моря и других систем континентального рифтинга // Литосфера. 2021. Т. 21. № 4. С. 469–490]. https://doi.org/10.24930/1681-9004-2021-21-4-469-490.

Baluev A.S., Moralev V.M., Glukhovskii M.Z., Przhijalgovskii E.S., Terekhov E.N., 2000. Tectonic Evolution and Magmatism of the Belomorian Rift System. Geotectonics 34 (5), 367–379.

Baluev A.S., Zhuravlev V.A., Przhiyalgovskii E.S., 2009. New Data on Structure of the Central Part of the White Sea Paleorift System. Doklady Earth Sciences 427, 891–896. https://doi.org/10.1134/S1028334X09060014.

Belashev B., Bakunovich L., Sharov N., Nilov M., 2020. Seismic Density Model of the White Sea's Crust. Geosciences 10 (12), 492. https://doi.org/10.3390/geosciences10120492.

Cheremisina Ye.N., Finkelstein M.Ya., Lyubimova A.V., 2018. GIS INTEGRO – Import Substitution Software for Geological and Geophysical Tasks. Geoinformatics 3, 8–17 (in Russian) [Черемисина Е.Н., Финкельштейн М.Я., Любимова А.В. ГИС INTEGRO – импортозамещающий программно-технологический комплекс для решения геолого-геофизических задач // Геоинформатика. 2018. № 3. С. 8–17].

Diuk V.A., Komashinsky V.I., Malygin I.G., 2018. Investigation of the Empirical Mode Decomposition Method in the Scenario of Acoustic Emission Signal Analysis. Information and Space 4, 50–55 (in Russian) [Дюк В.А., Комашинский В.И., Малыгин И.Г. Исследование метода эмпирической модовой декомпозиции в задаче анализа акустической эмиссии // Информация и космос. 2018. № 4. С. 50–55].

Dolgal A.S., Khristenko L.A., 2017. Application of Empirical Mode Decomposition in Processing Geophysical Data. Bulletin of the Tomsk Polytechnic University. Geo Assets Engineering 328 (1), 100–108 (in Russian) [Долгаль А.С., Христенко Л.А. Применение эмпирической модовой декомпозиции при обработке геофизических данных // Известия Томского политехнического университета. Инжиниринг георесурсов. 2017. Т. 328. № 1. С. 100–108].

Elsner J.B., Tsonis A.A., 1996. Singular Spectrum Analysis: A New Toolin Time Series Analysis. Plenum Press, New York, 164 p. https://doi.org/10.1007/978-1-4757-2514-8.

Gantmakher F.R., 2010. Matrix Theory. Fizmatlit, Moscow, 560 p. (in Russian) [Гантмахер Ф.Р. Теория матриц. М.: Физматлит, 2010. 560 с.].

Gavrilov A., 2013. Correlation Image Processing in Technical Vision Systems (in Russian) [Гаврилов А. Корреляционная обработка изображений в системах технического зрения, 2013]. Available from: https://pandia.ru/text/79/389/25136.php (Last Accessed November 15, 2022).

Golyandina N., Korobeynikov A., Shlemov A., Usevich K., 2015. Multivariate and 2D Extensions of Singular Spectrum Analysis with the Rssa Package. Journal of Statistical Software 67 (2), 1–78. https://doi.org/10.18637/jss.v067.i02.

Huang N.E., Samuel S.S.P. (Eds), 2005. Hilbert–Huang Transform and Its Applications. World Scientific Publishing Co, Singapore, 323 p. https://doi.org/10.1142/5862.

Kalinin D.F., Yanovskaya Yu.A., Dolgal A.S., 2019. Results of the Profile Complex Interpretation of Geopotential Fields through Empirical Mode Decomposition (EMD) Aimed at Oil-and-Gas Occurrence Prospects Assessment. Geophysics 1, 2–12 (in Russian) [Калинин Д.Ф., Яновская Ю.А., Долгаль А.С. Результаты профильной комплексной интерпретации геопотенциальных полей методом эмпирической модовой декомпозиции (ЕМД) с целью оценки перспектив нефтегазоносности // Геофизика. 2019. № 1. С. 2–12].

Kazanin G.S., Zhuravlev V.A., Pavlov S.P., 2006. Structure of the Sedimentary Cover and Petroleum Capacities of the White Sea. Drilling and Oil 2, 26–28 (in Russian) [Казанин Г.С., Журавлев В.А., Павлов С.П. Структура осадочного чехла и перспективы нефтегазоносности Белого моря // Бурение и нефть. 2006. № 2. С. 26–28].

Kazmin V.G., Byakov A.F., 1997. Continental Rifts: The Structural Control of Magmatism and Continental Breakup. Geotectonics 31 (1), 16–26.

Kearey Ph., Klepeis K.A., Vine F.J., 2009. Global Tectonics. Wiley-Blackwell, 482 p.

Kheraskova T.N., Sapozhnikov R.B., Volozh Yu.A., Antipov M.P., 2006. Geodynamics and Evolution of the Northern East European Platform in the Late Precambrian as Inferred from Regional Seismic Profiling. Geotectonics 6, 434–449. https://doi.org/10.1134/S0016852106060021.

Khutorskoy M.D., Akhmetzyanov V.R., Ermakov A.V., Leonov Yu.G., Podgornykh L.V., Polyak B.G., Sukhoi E.A., Tsybulya L.A., 2013. Geothermy of the Arctic Seas. GEOS, Moscow, 238 p. (in Russian) [Хуторской М.Д., Ахмедзянов В.Р., Ермаков А.В., Леонов Ю.Г., Подгорных Л.В., Поляк Б.Г., Сухих Е.А., Цыбуля Л.А. Геотермия Арктических морей. М.: ГЕОС, 2013. 238 с.].

Komarov A.G., 1965. Oceanic Ridges and Rift Structure. Geological Nature of Magnetic and Gravitational Anomalies above the Rift Valley. Priroda 7, 95–98 (in Russian) [Комаров А.Г. Океанические хребты и структура рифта. Геологическая природа магнитных и гравитационных аномалий над рифтовой долиной // Природа.1965. № 7. С. 95–98].

Korotchenko R.A., Semchenko A.N., Yaroshchuk I.O., 2013. Application of Multidimensional EOF Analysis in Geoinformatics. Digital Signal Processing 3, 17–20 (in Russian) [Коротченко Р.А., Семченко А.Н., Ярощук И.О. Применение многомерного ЕОФ анализа в геоинформатике // Цифровая обработка сигналов. 2013. № 3. С. 17–20].

Kutinov Yu.G., 2021. Modern Geodynamic Regime of the Arctic Crustal Segment and Oil Formation. Research and Publishing Center "Sociosphere", Penza, 281 p. (in Russian) [Кутинов Ю.Г. Современный геодинамический режим Арктического сегмента земной коры и нефтеобразование. Пенза: НИЦ Социосфера, 2021. 281 с.].

Lisitsyn A.P., Nemirovskaya I.A., Shevchenko V.P., Vorontsova V.G., 2017. The White Sea System. Vol. 4. The Processes of Sedimentation, Geology and History. Nauchny Mir, Moscow, 1030 p. (in Russian) [Лисицын А.П., Немировская И.А., Шевченко В.П., Воронцова В.Г. Система Белого моря: Процессы осадкообразования, геология и история. М.: Научный мир, 2017. Т. 4. 1030 с.].

Mitsyn S.V., Ososkov G.A., 2016. Finite Difference Method for Numerical Extrapolation of Grid Models of Geophysical Fields. Geoinformatics 3, 29–34 (in Russian) [Мицын С.В., Ососков Г.А. Экстраполяция сеточных моделей геофизических полей методом конечных разностей // Геоинформатика. 2016. №3. С. 29–34].

Navara A., Simoncini V., 2010. A Guide to Empirical Orthogonal Functions for Climate Data Analysis. Springer, Dordrecht, 152 p. https://doi.org/10.1007/978-90-481-3702-2.

Nilov M.Yu., Bakunovich L.I., Sharov N.V., Belashev B.Z., 2021. 3D Magnetic Crustal Model of the White Sea and Adjacent Areas. Arctic Ecology and Economy 11 (3), 375–385 (in Russian) [Нилов М.Ю., Бакунович Л.И., Шаров Н.В., Белашев Б.З. 3D магнитная модель земной коры Белого моря и прилегающих территорий // Арктика: экология и экономика. 2021. Т. 11. № 3. С. 375–385]. https://doi.org/10.25283/2223-4594-2021-3-375-385.

Priezzhev I.I., 2005. Constructing the Distribution of Physical Environment Parameters on the Basis of Gravity Prospecting and Magnetometric Data. Geophysics 3, 46–51 (in Russian) [Приезжев И.И. Построение распределений физических параметров окружающей среды по данным гравиразведки, магнитометрии // Геофизика. 2005. № 3. С. 46–51].

Raznitsin Yu.N., Gogonenkov G.N., Zagorovsky Yu.A., Trofimov V.A., Fedonkin M.A., 2020. Serpentinization of Mantle Peridotites as the Main Source of Deep Hydrocarbons of the West Siberian Oil and Gas Basin. Bulletin of Kamchatka

Regional Association "Educational-Scientific Center". Earth Sciences 45 (1), 66–88 (in Russian) [Разницин Ю.Н., Гогоненков Г.Н., Загоровский Ю.А., Трофимов В.А., Федонкин М.А. Серпентинизация мантийных перидотитов как основной источник глубинных углеводородов Западно–Сибирского нефтегазоносного бассейна // Вестник КРАУНЦ. Серия: Науки о Земле. 2020. Вып. 45. №1. С. 66–88]. https://doi.org/10.31431/1816-5524-2020-1-45-66-88.

Sharov N.V. (Ed.), 2022. Lithospheric Structure and Dynamics of the White Sea Region. KarRC RAS, Petrozavodsk, 239 p. (in Russian) [Строение и динамика литосферы Беломорья / Ред Н.В. Шаров. Петрозаводск: КарНЦ РАН, 2022. 239 с.].

Sharov N.V., Bakunovich L.I., Belashev B.Z., Nilov M.Yu., 2020a. Velocity Structure and Density Heterogeneities of the White Sea's Earth Crust. Arctic: Ecology and Economy 4 (40), 43–53 (in Russian) [Шаров Н.В., Бакунович Л.И., Белашев Б.З., Нилов М.Ю. Скоростная структура и плотностные неоднородности земной коры Белого моря // Арктика: экология и экономика. 2020. № 4 (40). С. 43–53]. https://doi.org/10.25283/2223-4594-2020-4-43-53.

Sharov N.V., Bakunovich L.I., Belashev B.Z., Zhuravlev V.A., Nilov M.Yu., 2020b. Geological-Geophysical Models of the Crust for the White Sea Region. Geodynamics & Tectonophysics 11 (3), 566–582 (in Russian) [Шаров Н.В., Бакунович Л.И., Белашев Б.З., Журавлев В.А., Нилов М.Ю. Геолого-геофизические модели земной коры Беломорья. Геодинамика и тектонофизика. 2020. Т. 11. № 3. С. 566–582]. https://doi.org/10.5800/GT-2020-11-3-0491.

Sharov N.V., Slabunov A.I., Isanina E.V., Krupnova N.A., Roslov U.V., Chipzova N.I., 2010. Seismological Cross-Section of the Earth's Crust along the Profile DSS – CMP "Land – Sea" Kalevala – Kem' – the White Sea Neck. Geophysical Journal 32 (5), 21–34 (in Russian) [Шаров Н.В., Слабунов А.И., Исанина Э.В., Крупнова Н.А., Рослов Ю.В., Щипцова Н.И. Сейсмический разрез земной коры по профилю ГСЗ-ОГТ «Суша-море» Калевала – Кемь – горло Белого моря // Геофизический журнал. 2010. Т. 32. № 5. С. 21–34].

State Geological Map of the Russian Federation, 2009a. Baltic Series. Scale 1:1000000. Sheet Q-(35), 36 (Apatity). Explanatory Note. VSEGEI, Saint Petersburg, 487 p. (in Russian) [Государственная геологическая карта Российской Федерации. Серия Балтийская. Масштаб 1:1000000. Лист Q-35, 36 (Апатиты): Объяснительная записка. СПб.: ВСЕГЕИ, 2009. 487 с.].

State Geological Map of the Russian Federation, 2009b. Baltic Series. Scale 1:1000000. Sheet Q-37 (Arkhangelsk). Explanatory Note. VSEGEI, Saint Petersburg, 338 p. (in Russian) [Государственная геологическая карта Российской Федерации. Серия Балтийская. Масштаб 1:1000000. Лист Q-37 (Архангельск): Объяснительная записка. СПб.: ВСЕГЕИ, 2009. 338 с.].

State Geological Map of the Russian Federation, 2009c. Mezen series. Scale 1:1000000. Sheet Q-38 (Mezen). Explanatory Note. VSEGEI, Saint Petersburg, 350 p. (in Russian) [Государственная геологическая карта Российской Федерации. Серия Мезенская. Масштаб 1:1000000. Лист Q-38 (Мезень): Объяснительная записка. СПб.: ВСЕГЕИ, 2009. 350 с.].

Statistics Toolbox for Use with Matlab, 2005. User's Guide. Version 5. Math Works, 912 p.

Stepanov V.S., Stepanova A.V., 2007. Basic and Ultrabasic Rocks of the Razostrov Island, the White Sea. In: Geology and Minerals of Karelia. Vol. 10. KarRC RAS, Petrozavodsk, p. 16–26 (in Russian) [Степанов В.С., Степанова А.В. Основные и ультраоснвные породы Разострова, Белое море // Геология и полезные ископаемые Карелии. Петрозаводск: КарНЦ РАН, 2007. Вып. 10. С. 16–26].

Tevelev Ark.V., Fedorovsky A.S., 2016. Transfer Zones in the Baikal Rift Structure. In: Tectonics, Geodynamics and Ore Formation of Fold Belts and Platforms. Proceedings of XLVIII Tectonic Conference (February 1–6, 2016). Vol. 2. GEOS, Moscow, p. 214–218 (in Russian) [Тевелев Арк.В., Федоровский А.С. Трансферные зоны в структуре Байкальского рифта // Тектоника, геодинамика и рудогенез складчатых поясов и платформ: Материалы XLVIII тектонического совещания (1–6 февраля 2016 г.). М.: ГЕОС, 2016. Т. 2. С. 214–218].

Tsibulua L.A., Levashkevich V.G., 1992. Terrestrial Heat Flow in the Barents Sea Region. KSC RAS, Apatity, 115 p. (in Russian) [Цыбуля Л.А., Левашкевич В.Г. Тепловое поле Баренцевоморского региона. Апатиты: КНЦ РАН, 1992. 115 с.].

Wasilewski P.J., Mayhew M.A., 1992. The Moho as a Magnetic Boundary Revisited. Geophysical Research Letters 19 (2), 2259–2262. https://doi.org/10.1029/92GL01997.

Zhuravlev V.A., 2007. The Crustal Structure of the White Sea Region. Prospect and Protection of Mineral Resources 9, 22–26 (in Russian) [Журавлев В.А. Структура земной коры Беломорского региона // Разведка и охрана недр. 2007. № 9. С. 22–26].